

NUMERICAL ANALYSIS OF POLYMERIC HEATSINKS

Lourenço Bastos^{1*}, Ângelo Marques¹, Bruno Vale¹, Ricardo Freitas¹, Susana Silva², Aníbal Portinha², Pedro Bernardo², Gustavo Dias³ and Filipa Carneiro¹

¹PIEP - Centre for Innovation in Polymer Engineering, Universidade do Minho Campus de Azurém, 4800-058, Guimarães, Portugal

² Bosch Car Multimedia, Rua Max Grundig, 35, 4705-820, Braga, Portugal

³ IPC – University of Minho Campus de Azurém, 4800-058, Guimarães, Portugal

*Corresponding Author: lourenco.bastos@piep.pt

ABSTRACT

This work focused on the study of geometries for polymeric heatsinks that would lead to better thermal dissipation behavior. Firstly, typical heatsink geometries were studied, in order to analyze the influence of the number of fins and their surface area, fin thickness and height, on thermal dissipation. Moreover, taking advantage of the fact that polymers are easier to process, more complex geometries (some more suited to additive manufacturing) were analyzed. In a second phase, to better analyze the influence of heatsink geometry on the thermal dissipation capacity, some of the heatsink analyzed in the preliminary phase were applied to a more realistic case of a complex light electronic enclosure. As conclusion, it was observed that the replacement of traditional metal heatsinks by polymeric ones in electronic devices is possible, if adequate changes are made to the electronic devices, in order to optimize fluid dynamics and consequently heat dissipation. An acceptable thermal behavior of polymeric heatsink may be achievable, with an adequate optimization of heatsink geometry, either by optimizing fin thickness, height and number or orienting heatsink fins towards guiding the air flow to critical areas.

1 INTRODUCTION

With the recent continuous development of electronic devices towards higher performance and the constant demand for increasingly smaller and lighter solutions, the heat dissipation problem has become a major obstacle to the development of new products (Ahmed *et al.*, 2018; Ong and KuShaari, 2020). Heatsinks are one of the most used devices to effectively absorb or dissipate heat from the surroundings (air) using extended surfaces such as fins and spines (Lee, 2017). Thus, the necessity to further explore their capacity and possibilities to make them smaller and lighter. The use of polymeric materials in heatsinks have been analyzed for such purpose.

Polymeric materials, despite having a considerably lower heat dissipation capacity than commonly used metals, offer great advantages over metals such as high corrosion resistance, high strength to weight ratio, low cost (Cevallos *et al.*, 2012) and the ease of processing. Moreover, some studies even indicate that an adequate thermal dissipation capacity, for cooling electronic devices, can be achieved through different methods (Marchetto *et al.*, 2019).

Two main approaches to improve the heat conduction of polymers are found in the literature. The first consists on optimizing the heatsink geometry in order to increase its thermal conduction capacity, for example by reducing the thickness of the heat sink walls (Glade, Moses and Orth, 2017; Deisenroth *et al.*, 2018), which also leads to the need to analyze complex geometries, creating microchannels in the heatsink (Marchetto *et al.*, 2019) or increasing the number of fins, in order to maximize the surface area of the heatsink which, generally, enhances its capacity to dissipate heat.

The other approach involves the inclusion of thermally conductive fillers/materials in the polymer matrix in order to improve the overall heat conduction. Regarding this topic, the work of Marchetto *et*

al. (2019) presents review with various materials already studied in the literature and applied to heatsinks, such as PA with different fillers (Heinle and Drummer, 2010; Cho *et al.*, 2016), Epoxy with different fillers (Chen *et al.*, 2003; Lee *et al.*, 2013), PPS+Graphite (Bahadur and Bar-Cohen, 2004, 2005, 2007; Icoz and Arik, 2010) and others (Lee *et al.*, 2004; Kang *et al.*, 2005; Koşar, 2010; Koyuncuoğlu, Okutucu and Külâh, 2010). Moreover, there is some studies that, similarly to this study, use graphite to enhance the thermal behavior of polymeric heatsink, such as the works of Norley *et al.* (2001), Chen *et al.* (2003), Marotta *et al.* (2003), Bahadur and Bar-Cohen (2004) (2005) (2007), Smalc *et al.* (2005) and Icoz and Arik (2010).

From these studies, heatsinks with rectangular fins seem to be the most common (Norley *et al.*, 2001; Chen *et al.*, 2003; Marotta *et al.*, 2003; Heinle and Drummer, 2010; Icoz and Arik, 2010; Cho *et al.*, 2016), with some studies using pin fins (Bahadur and Bar-Cohen, 2004, 2005, 2007), and others using microchannels (Lee *et al.*, 2004; Kang *et al.*, 2005; Koşar, 2010; Koyuncuoğlu, Okutucu and Külâh, 2010). In the work of Waheed *et al.* (2019) different heatsink geometries are analyzed, some of them being more complex and only suited for additive manufacturing. Similarly, some studies analyze different metal heatsink geometries, both conventional and more complex, such as the works of Wong *et al.* (2009), Dede *et al.* (2015), Joo and Kim (2015), Subramaniam *et al.* (2018) and Nafis *et al.* (2021)

2 MATERIALS AND METHODS

In this study, a numerical approach was used to analyze the influence of the heatsink geometry, i.e. the width, the height and the number of fins, on the thermal behavior of an enclosure for an electronic device. In a preliminary analysis, a simple case of an heatsink in contact with five heat sources, placed in a simplified PCB (Printed Circuit Board), was considered in order to evaluate which heatsink configurations would lead to better thermal performance. A simple enclosure that surrounds these geometries was also considered. Moreover, different approaches for the fin geometry were also studied, such as considering wave fins, curving the fins at the flow entrance, using pins instead of fins and considering complex pins, more suited to be produced with additive manufacturing.

This study establishes a baseline for heatsink geometry optimization by analyzing various fin geometries in a simple enclosure. The thermal performance is compared to Costa *et al.* (2024) who investigates a more complex enclosure with a heatsink with rectangular fins. In addition to this previous work, different fin geometries and their optimization process are explored, suggesting that alternative designs might be more effective.

2.1 Mathematical equations

The numerical simulations were performed using the commercial software Fluent®, from the Ansys software suite (Ansys, Inc., Canonsburg, PA, USA), considering the k-ε Turbulent Model with Enhanced Wall Treatment algorithm and a convergence criterion of 1E-5. This software solves the three-dimensional equations for mass, Equation (1), momentum, Equation (2), and heat transfer, Equation (3), assuming conservation for each variable:

$$\nabla \vec{v} = 0 \quad (1)$$

$$\frac{\partial}{\partial t}(\rho \vec{v}) + \nabla(\rho \vec{v} \vec{v}) = \nabla p + \nabla(\bar{\tau}) \quad (2)$$

$$\frac{\partial}{\partial t}(\rho E) + \nabla[\vec{v}(\rho E + p)] = \nabla(k_{eff} \nabla T) + S_h, \quad E = h - \frac{p}{\rho} + \frac{v^2}{2} \quad (3)$$

Where \vec{v} is the fluid velocity vector, ρ is the density, p is the static pressure, $\bar{\tau}$ is the stress tensor, k_{eff} is the effective conductivity, and S_h other heat sources. The turbulence model is described by Equations (4) and (5):

$$\frac{\partial}{\partial t}(\rho k) + \nabla(\rho \vec{v} k) = \nabla \left[\left(\mu + \frac{\mu_t}{\sigma_k} \right) \frac{\partial k}{\partial x_j} \right] + G_k - \rho \varepsilon, \quad \mu_t = \rho C_\mu \frac{k^2}{\varepsilon} \quad (4)$$

$$\frac{\partial}{\partial t}(\rho \varepsilon) + \nabla(\rho \vec{v} \varepsilon) = \nabla \left[\left(\mu + \frac{\mu_t}{\sigma_\varepsilon} \right) \frac{\partial \varepsilon}{\partial x_j} \right] + C_{1\varepsilon} \frac{\varepsilon}{k} G_k - C_{2\varepsilon} \rho \frac{\varepsilon^2}{k} \quad (5)$$

where k is the kinetic energy, ε the dissipation rate, μ the viscosity, and μ_t the turbulent (or eddy) viscosity. G_k represents the generation of turbulence kinetic energy due to the mean velocity gradients. $C_{1\varepsilon}$, $C_{2\varepsilon}$ and C_μ are constants, 1.44, 1.92 and 0.09, respectively. $\sigma_k = 1.0$ and $\sigma_\varepsilon = 1.3$ are the turbulent Prandtl numbers for k and ε , respectively. Furthermore, radiation was not applied in the simulation, as it was considered neglectable when compared to forced convection.

2.2 Geometrical model

For the preliminary study, as mentioned before, a simple case of an heatsink in contact with 5 heat sources was considered. The heat sources were simplified to simple square shaped boxes with 15mm of length and 2.5mm of height. The dimensions of the remaining geometries are presented in Figure 1, where the geometrical model considered for the numerical simulation can be observed. Figure 2 presents the other heatsink geometries that are being analyzed. To note, that a thin layer (0,5mm) of gap filler is considered between the heatsink and the heat sources. Table 1 presents the heatsink geometries that were analyzed in this preliminary study.

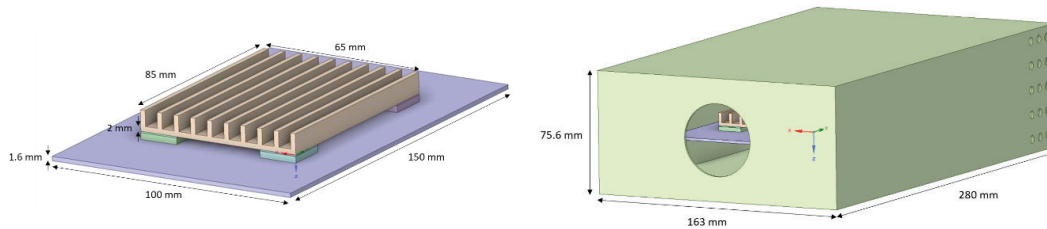


Figure 1: Geometrical model for the preliminary study.

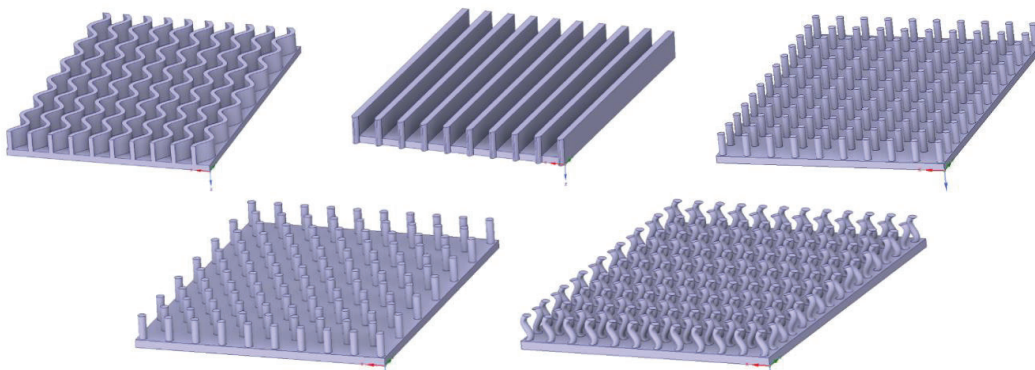


Figure 2: Geometrical model for the proposed fin/pin configurations.

For the realistic case study, an enclosure with similar outer dimensions is considered, being that the PCBs and heatsink have similar global dimensions as the ones presented above. However, the whole enclosure is much more complex, having 62 heat sources, 3 heatsinks and 3 PCBs, as described by Costa *et al.* (2024). The geometrical model used for the numerical simulations in this case are presented in Figure 3.

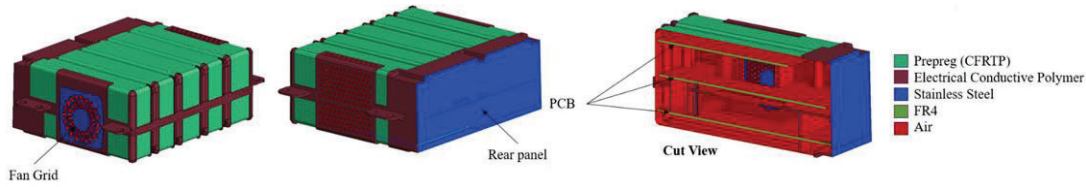


Figure 3: Geometrical model for the case study (Costa *et al.*, 2024).

2.3 Geometric domain discretization

The discretization of the geometric domain in small control volumes, or mesh generation, is a crucial step in a numerical analysis. When the mesh generation process is adequate, the numerical algorithm becomes more robust and efficient and, consequently, a more realistic and accurate solution is achieved. Thus, a mesh independence study was performed for the rectangular heatsink with 10 fins with a thickness of 2 mm and a height of 6 mm, for a global element size of 5, 3, 2 and 1 mm.

For the preliminary study, having in mind the results obtained in the mesh independence study, the meshes created for the solids have hexahedron elements (8 nodes) with a global size of 1 mm, being that in the fins the size of the elements varied with each case, to ensure that there are at least 3 elements throughout the thickness of the fins. As for the air flowing inside the enclosure, a mesh with tetrahedron (4 nodes) and wedge (6 nodes) elements was created with a global size of 2 mm, being that in the proximity of other volumes the mesh is refined to 0.7 mm. In Table 1 are presented the number of elements for the meshes created and Figure 4 presents a section view from one of the meshes and the results of the mesh independence study (Max. Temperature vs. Number of elements).

Table 1: Geometrical parameters for the analyzed heatsinks

| | Fin thickness (mm) | Fin height (mm) | Number of fins/pins | Heatsink surface area (mm ²) | Number of elements in the mesh |
|--|--------------------|-----------------|---------------------|--|--------------------------------|
| Typical heatsink with rectangular fins | | No fins | | 11650 | 1722465 |
| | 2 | 6 | 2 | 13738 | 3522872 |
| | | | 4 | 15826 | 3556302 |
| | | | 10 | 22090 | 3794822 |
| | | | 16 | 28354 | 3937727 |
| | | | 22 | 34618 | 5168253 |
| | 0.4 | | | 21898 | 4954326 |
| | 1 | 6 | 10 | 21970 | 3837869 |
| | 3 | | | 22210 | 3764100 |
| | 4 | | | 22330 | 3690045 |
| | | | | 13390 | 3389909 |
| | 2 | 1 | 10 | 15130 | 3498689 |
| | | 2 | | 29050 | 4136529 |
| | | 10 | | 46450 | 4925467 |
| | 0.4 | 6 | 20 | 32146 | 5635542 |
| 30 | | | 42394 | 7018650 | |
| 40 | | | 45925 | 8364790 | |
| Heatsink with rounded fins | | | 10 | 22267.89 | 4456121 |
| Heatsink with wave fins | | | | 24046 | 5372667 |
| Heatsink with pins | 2 | 6 | 130 (pins) | 13500 | 5830666 |
| Heatsink with misaligned pins | | | 124 (pins) | 13387.34 | 5750099 |
| Heatsink with curved pins | | | 130 (pins) | 14239 | 6915986 |

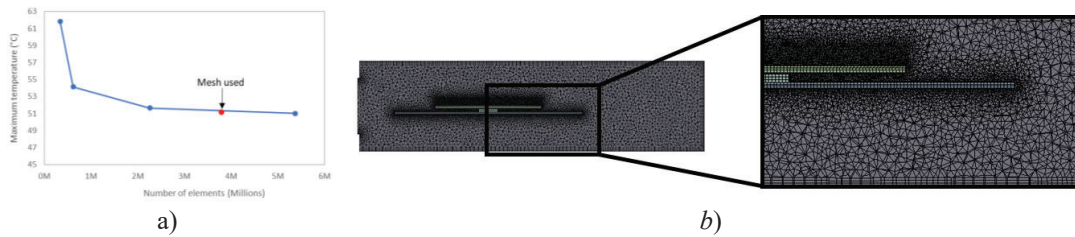


Figure 4: Mesh created for the preliminary study: a) Mesh independence study; b) Section view of the meshes created for the numerical simulations.

Table 2 presents the properties of the meshes created for the numerical simulations of the case study. Moreover, in the work of Costa *et al.* (2024), a section view of the mesh created can be observed.

Table 2: Properties of the mesh created for the case study (Costa *et al.*, 2024).

| Material | Type | Element Size |
|----------|------------------------------|--|
| Solids | PCBs | Hexahedrons (8 Nodes) |
| | | In-plane: 1.5 mm Through plane: 0.6 mm |
| | Heatsinks | Tetrahedrons (4 Nodes) |
| | Gap fillers and heat sources | Hexahedrons (8 Nodes) |
| | | Global: 0.7 mm with proximity of 0.5 mm |
| | | Global: 0.8 mm |
| | | Thickness: 0.2 mm |
| | Enclosure | Tetrahedrons (4 Nodes) |
| | | Global: 1.5 mm |
| Fluids | Air | Tetrahedrons (4 nodes) and Wedge elements for the boundary layer (6 Nodes) |
| | | Boundary layer: 3 layers, 0.2 mm for the first layer and growth rate of 1.2 Global: Tetrahedrons, 1.5 mm with proximity of 0.5 mm |

2.4 Materials

The same materials are considered for both cases (preliminary study and case study) and are based in the properties used by Costa *et al.* (2024). The properties of the materials considered in the numerical simulation are presented in Table 3. Furthermore, air viscosity was considered as 1.79E-05 kg/m.s.

Table 3: Material properties

| Material | Density (kg/m ³) | Thermal conductivity (W/m°C) | Specific heat (J/kg°C) |
|---|------------------------------|---|---|
| Aluminum | 2650 | 140 | 896 |
| Electrically conductive polymer (Enclosure) | 1360 | 0.2 | 1500 |
| Thermal conductive polymer (heatsinks) | 1850 | In-plane: 20 Through plane: 6 | 50 °C – 1180 85 °C – 1250 130 °C – 1330 |
| Gap Filler | 3100 | 3.5 | 800 |
| PCB (50%FR4-50%Cu) | 4500 | 200 | 385 |
| CFRTP (Only used in the case study) | 1500 | In-plane (x e y): 2.5 Through plane (z): 0.6 | 25 °C – 900 120 °C – 1291 200 °C – 1466 |
| Air | 20°C – 1.204 | 20°C – 0.0242 | 1006.43 |
| | 50°C – 1.093 | 50°C – 0.0262 | |
| | 80°C – 1.000 | 80°C – 0.03 | |
| | 125°C – 0.887 | 125°C – 0.0336 | |

2.5 Boundary conditions

The case study boundary conditions were applied according to the work developed by Costa *et al.* (2024). Thus, for the air flowing inside the enclosure, the action of the fan cooling the device was defined by a fan surface condition, considered in the surface identified in Figure 5a. This condition is defined by a polynomial function that describes the characteristic curve of the fan or P-Q curve (Figure 5b). Furthermore, at the inlet, a turbulent intensity of 20% and turbulent viscosity ratio of 10 were defined. Moreover, a pressure outlet condition was considered at the surface identified in Figure 5c, with a gauge pressure of 0 MPa, a backflow turbulent intensity of 5% and a backflow turbulent viscosity ratio of 10.

Regarding the conditions at the exterior of the enclosure, convection is applied in all the outer walls to simulate the air surrounding the enclosure, being defined a heat transfer coefficient of 10 W/m²°C for a free stream temperature of 65 °C.

Finally, all the heat sources were considered to be active and generating heat and the power applied by each heat source is in accordance with the ones presented by Costa *et al.* (2024).

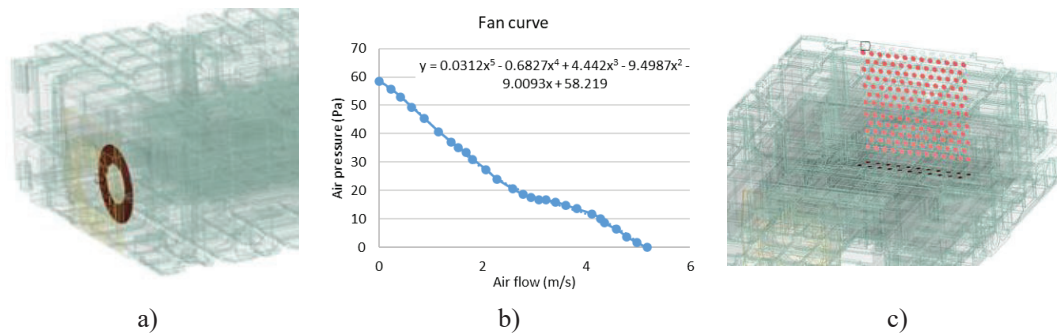


Figure 5: Flow conditions in the study case (Costa *et al.*, 2024): a) Fan surface; b) Fan P-Q curve; c) Outlet surfaces.

The boundary conditions applied in the preliminary study were based in the conditions of the study case, although they were simplified, or changed a bit, to allow a faster setup of the numerical models and lower simulation time, consequently allowing the analysis of more geometrical changes.

Regarding the air flow, similar inlet and outlet conditions were applied in the preliminary study. However, the outlet surface was considerably changed (Figure 6), so a worse airflow would be obtained. Furthermore, for the conditions at the exterior of the enclosure, it was defined that there is no heat flux in the outer walls, instead of considering convection. Both of these changes were done since the outside temperature was changed to a considerably lower one (20°C), which would lead to considerably lower temperatures and to a less noticeable influence of the geometric changes done to the heatsinks on the temperatures observed in the enclosure. This change in temperature was considered because in the future it is pretended to experimentally validate this study and having an outside temperature around 20°C is much easier to replicate, even considering the insulated outer walls. Moreover, as mentioned before, only five heat sources were considered in this simplified case, with a power of 45 W each.

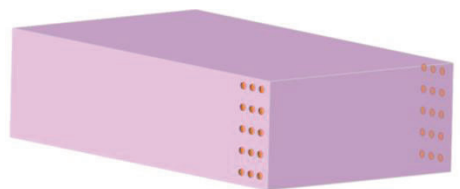


Figure 6: Outlet surface for the preliminary study.

3 Results and discussion

3.1 Preliminary study

Starting with the results obtain in the analysis of a typical heatsink with rectangular fins, as mentioned before, the geometry of the fins was studied, namely the number of fins, fin thickness and the fin height. Moreover, the results were analyzed by observing the maximum temperature reached inside the enclosure. In Figure 7 are presented the results obtained by varying each of these geometrical variables.

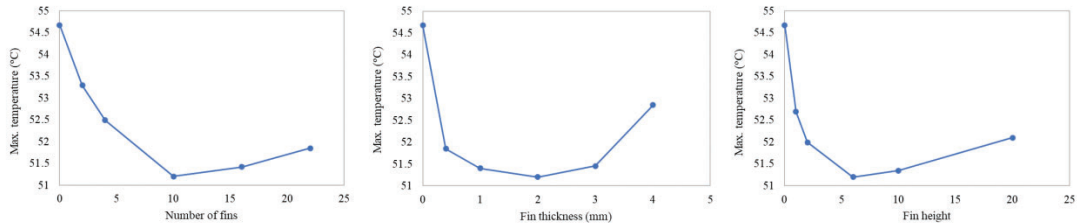


Figure 7: Influence of geometrical changes in the maximum temperature observed in heatsinks with rectangular fins.

Starting with the variation of the number of fins, it is possible to observe that increasing the number of fins is beneficial, promoting a decrease of the maximum temperature observed, to a certain point, in this case 10/16 fins. Although the heatsink surface area is increasing, a further increase in the number of fins seems to promote an increase in the maximum temperature observed. This might be related to the fact that the space between fins is decreasing and the heatsink starts to work as an insulator.

As for the fin thickness, a similar tendency is observed, i.e. an increase in fin thickness is beneficial until the value of 2 mm is reached. From this point on, the temperature increases and, again, the heatsink starts to work as insulation.

Regarding the fin height, the same tendency is observed, an increase in fin height promotes a decrease in the maximum temperature, reaching the lowest temperature for 6 mm of height. Higher fins promote an increase in temperature.

Having these results in mind, it can be concluded that an increase in heatsink surface area might not always be beneficial for the capacity to dissipate heat. Furthermore, maintaining an adequate spacing between fins is essential for the heatsink capacity to dissipate heat. Thus, the strategy of decreasing the fin thickness as much as possible is usually adopted, in order to overcome the space limitation. Since decreasing the fin thickness to 0.4 mm does not seem to drastically increase the maximum temperature (0.4 mm – 51.85 °C; 2 mm – 51.2 °C), this decrease should allow adding a considerable number of fins without compromising the fin spacing. Therefore, a second study was also conducted considering a fin thickness of 0.4 mm and a fin height of 6 mm to analyze the influence of the increase in fin number for this case. The results obtained in this study are presented in Figure 8.

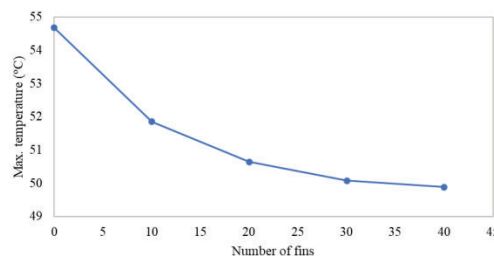


Figure 8: Influence of the number of fins for an heatsink with a fin thickness of 0.4 mm.

As can be seen, reducing the fin thickness allows adding more fins without negatively affecting the heatsink capacity to dissipate heat and compensates for the temperature increase due to the decrease in thickness as observed previously. In this case it is possible to obtain a considerably lower temperature (49.88 °C) than the best one observed in the previous study (51.20 °C). Observing the tendency of the obtained results, it is not expected that a further increase in the number of fins would promote a considerable decrease in temperature.

Thus, a decrease in fin thickness might not be directly beneficial for the capacity to dissipate heat but allows a better use of heatsink space, allowing the addition of a greater number of fins without affecting the adequate spacing between fins and promoting a higher capacity to dissipate heat.

Now analyzing other types of heatsink geometries, as mentioned before, five other heatsink geometries were analyzed. Having in mind the results obtained in the previous studies, a fin/pin thickness of 2 mm and a height of 6 mm were considered. A thickness of 0.4 mm should be more adequate, as observed before, but it requires a higher computational effort, so a thickness of 2 mm was chosen to simplify the creation of numerical models and allow faster simulations. Despite this, the same tendencies/conclusions should be achieved. In Table 4 are presented the results obtained for these heatsink geometries.

Table 4: Maximum temperature obtained for different heatsink geometries

| | Number of fins | Heatsink Surface area (mm ²) | Weight (g) | Max. Temperature (°C) |
|---------------------------|----------------|--|------------|-----------------------|
| Metal heatsink | 10 | 22090 | 56.31 | 48.68 |
| Baseline | | 22090 | 39.31 | 51.20 |
| Rounded fins | 10 | 22267.89 | 39.61 | 50.95 |
| Polymeric heatsink | | | | |
| Wave fins | | 24046 | 36.99 | 50.03 |
| Pins | 130 | 13500 | 24.98 | 51.55 |
| Misaligned pins | 124 | 13387.34 | 24.77 | 50.61 |
| Curved pins | 130 | 14239 | 26.34 | 50.36 |

As can be observed, for this simplified case, using a polymeric heatsink, instead of a metallic one, promotes an increase of 2.52 °C in the maximum temperature, which might not seem that considerable, but it is the biggest difference observed in all the results obtained for the simplified case.

Using rounded fins at the entrance of the air flow in the heatsink seems to contribute to a decrease in the maximum temperature observed, as it promotes a better air flow and less air stagnation in this area.

Using wavy fins also seems to be beneficial to the heat dissipation capacity, with a greater decrease in the maximum temperature, when compared to using rounded fins. This was expected, since the wavy fins promote more air turbulence in the heatsink, which is usually beneficial for dissipating heat.

Regarding the use of pins instead of fins, it seems to slightly increase the maximum temperature. However, observing the considerable decrease in weight, with just a slight increase in temperature, this change might be beneficial if weight is a critical factor to take into account.

Even better is the result for the case considering misaligned pins, where the surface area is further decreased and the maximum temperature is also decreased – a temperature similar to the heatsink with rounded fins is achieved. This follows the same principal observed in the case with wavy fins, where the turbulence around the heatsink is increased, which promotes a better heat dissipation capacity.

Finally, the last studied geometry is similar the previous one but uses twisted pins, in order to increase surface area and turbulence around the heatsink. This case presented the lowest temperature of the studied geometries until this point, but is also the most complex geometry, being more suited to be produced by additive manufacture.

3.2 Case study

Following the results obtained in the preliminary study, a more realistic case was analyzed in order to better observe the influence of the fin geometry on the temperature of an electronic device enclosure. Thus, some of the heatsink geometries studied before were applied in this case study, namely the results obtained by Costa *et al.* (2024), corresponding to the best heatsink geometry obtained in the first preliminary study, the best overall geometry (obtained in the second preliminary study, with a fin thickness of 0.4 mm and 40 fins) and the worst overall geometry (heatsink without fins). Figure 9a shows an outer view of the temperature distribution obtained in the enclosure and Figure 9b shows the temperature distribution for a section plane, passing through the middle of the enclosure.

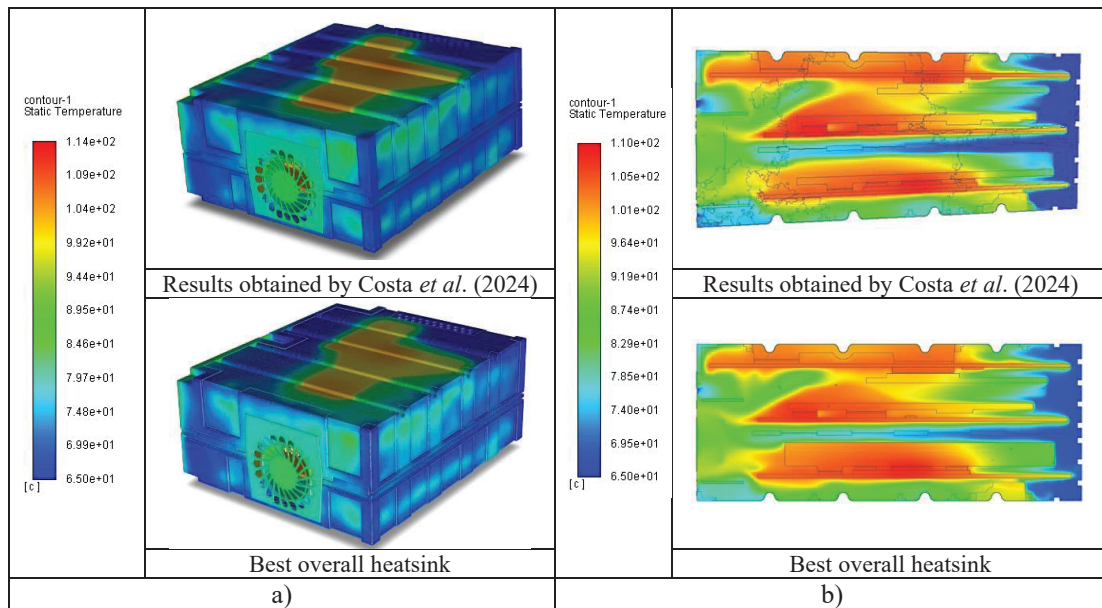


Figure 9: Temperature distribution in the enclosure (a) and (b) the temperature distribution in a section plane, for both the best heatsink from the first preliminary study, obtained by Costa *et al.* (2024), and the best overall heatsink.

In Table 5 are presented the maximum temperatures obtained in the case study.

Table 5: Maximum temperatures obtained in the case study

| | Metal Heatsink | Polymeric heatsink | | |
|------------------------------|----------------|--|-----------------------|------------------------|
| | | Results obtained by Costa <i>et al.</i> (2024) | Best overall heatsink | Heatsinks without fins |
| Air | 97.14 | 113.66 | 110.69 | 208.92 |
| Enclosure | 94.72 | 104.16 | 105.34 | 126.58 |
| Bottom heatsink | 94.01 | 109.03 | 108.79 | 116.14 |
| Intermediate heatsink | 96.15 | 112.39 | 110.57 | 211.15 |
| Top heatsink | 95.22 | 107.24 | 105.60 | 116.40 |
| PCB C | 94.6 | 109.52 | 108.55 | 117.43 |
| PCB B | 97.18 | 113.20 | 110.27 | 209.72 |
| PCB A | 96.77 | 110.07 | 107.70 | 195.14 |

As can be seen, comparing the results obtained by Costa *et al.* (2024) and the results obtained with the heatsink without fins, it is possible to observe a much more considerable difference in the maximum temperature, when comparing with the simplified case, where a difference of only 3.47 °C was observed

(best typical heatsink – 51.20 °C; heatsink without fins – 54.67 °C). This was expected, since the air flow is much worse in this case, even when the outlets of the simplified case were changed to worsen the air flow. In this case, the air flow is much more limited due to all the components inside the enclosure, with much less place for the air to flow around.

Moreover, similarly to what was observed in the simplified case, for the best overall heatsink (with a fin thickness of 0.4 mm and 40 fins) a lower maximum temperature is observed, when compared to the best typical heatsink (with rectangular fins). Here, a more significant difference in temperature (2.97°C) is again observed for this case study, when compared to the simplified case where a difference of 1.32°C was observed for the maximum temperature.

Finally, the use of a polymeric heatsink, instead of a metallic one, in a more realistic case promotes a much more significant difference (16.52 °C) in the maximum temperature observed, similarly to what is observed for the previously discussed results. As expected, the use of a polymeric heatsink promotes a considerable increase in the temperature observed. Nevertheless, changing the original metallic enclosure and heatsinks by polymeric ones allowed a considerable weight reduction of 33%. Moreover, even with the considerable increase in the temperatures observed, the temperatures observed for each component were considered to not impose any problems for the correct function of the electronic device (Costa *et al.*, 2024): “Notably, certain components exhibited elevated temperatures in simulations, which were deemed non-problematic since the scenario – simultaneous operation of all heat sources – assumed a condition unlikely to occur in reality.”

4 Conclusions

In this work, a study was conducted to evaluate the influence of the heatsink geometry, namely the thickness, height and number of fins, on the thermal dissipation behavior of an electronic enclosure. Analyzing the results obtained in the preliminary studies, it was possible to observe that increasing the increasing heatsink area does not always promote a better heat dissipation capacity and that an adequate spacing between heatsink fins is essential for a good heat dissipation capacity. Furthermore, separately increasing the height, thickness or the number of fins is beneficial to a certain point, from which the heat dissipation capacity of the heatsink starts to decrease and the heatsink starts to behave as an insulator. Lastly, decreasing the fin thickness might not be directly beneficial for the capacity to dissipate heat, but allows a better use of heatsink space, allowing the addition of a greater number of fins without affecting the adequate spacing between them and, consequently, promoting a higher capacity to dissipate heat.

Regarding the case study, the changes in heatsink geometry have a more considerable impact in the temperatures observed. Moreover, the same tendencies observed in the preliminary studies are again observed in the case study, namely: Using an heatsink with no fins promotes a great increase in the temperature observed; Using the best heatsinks from the preliminary study still promote an increase in temperature, but the thermal behavior is much more similar to the one observed with metal heatsinks - a difference of 16.5 °C is observed for the heatsink with fin thickness of 2 mm, a fin height of 6mm and 10 fins. The heatsink with fin thickness of 0.4 mm and 40 fins presented the best behavior observed from the polymeric heatsinks, with a difference of 13.44 °C to the metal heatsink. Even with this increase in temperature, changing the original metallic enclosure and heatsinks by polymeric ones allowed a considerable weight reduction and the temperatures observed for each component were considered to not impose any problems for the correct function of the electronic device.

To conclude, an adequate optimization of the heatsink geometry, in electronic devices, is of utmost importance to guarantee the best possible thermal dissipation behavior, especially in the case of polymeric heatsinks due to their low thermal dissipation capacity. Furthermore, the use of polymeric heatsink, instead of metallic ones, should be feasible if adequate optimizations are done to both the heatsinks and the enclosure. For situations where weight is a critical factor to take into account, the use of a polymeric heatsink might be beneficial, despite the fact that thermal dissipation will be worsened.

REFERENCES

- Ahmed, H. E., Salman, B. H., Kherbeet, A. S., Ahmed, M. I., 2018, 'Optimization of thermal design of heat sinks: A review', *International Journal of Heat and Mass Transfer*. Elsevier Ltd, 118, pp. 129–153. doi: 10.1016/j.ijheatmasstransfer.2017.10.099.
- Bahadur, R. and Bar-Cohen, A., 2004, 'Thermal design and optimization of staggered polymer pin fin natural convection heat sinks', *Thermomechanical Phenomena in Electronic Systems -Proceedings of the Intersociety Conference*, 1(2), pp. 268–275. doi: 10.1109/itherm.2004.1319184.
- Bahadur, R. and Bar-Cohen, A., 2005, 'Thermal performance limits of polymer composite pin fin heat sinks', *Proceedings - Electronic Components and Technology Conference*. IEEE, 2, pp. 1720–1727. doi: 10.1109/ectc.2005.1442025.
- Bahadur, R. and Bar-Cohen, A., 2007, 'Orthotropic thermal conductivity effect on cylindrical pin fin heat transfer', *International Journal of Heat and Mass Transfer*, 50(5–6), pp. 1155–1162. doi: 10.1016/j.ijheatmasstransfer.2006.04.025.
- Cevallos, J. G., Bergles, A. E., Bar-Cohen, A., Rodgers, P., Gupta, S. K., 2012, 'Polymer heat exchangers-history, opportunities, and challenges', *Heat Transfer Engineering*, 33(13), pp. 1075–1093. doi: 10.1080/01457632.2012.663654.
- Chen, G., Capp, J., Getz, G., Flaherty, D. Norley, J., 2003, 'OPTIMUM DESIGN OF HEAT SINKS USING NON-ISOTROPIC GRAPHITE COMPOSITES', *ASME Summer Heat Transfer Conference*, pp. 1–6.
- Cho, E. C., Huang, J., Li, C., Chang-Jian, C., Lee, K., Hsiao, Y., Huang, J., 2016, 'Graphene-based thermoplastic composites and their application for LED thermal management', *Carbon*. Elsevier, 102, pp. 66–73. doi: 10.1016/j.carbon.2016.01.097.
- Costa, S., Bastos, L., Rietter, L., Oliveira, R., Freitas, R., Rocha, A., Vale, B., Ribeiro, C., Serrão, D., Silva, J., Gonçalves, N., Carneiro, F., Silva, S., Portinha, A., Bernardo, P., Dias, G., 2024, 'Numerical simulation and 1 experimental evaluation for the development of a light electronic enclosure used in automotive industry', in *European Congress on Computational Methods in Applied Sciences and Engineering*.
- Dede, E. M., Joshi, S. N. and Zhou, F., 2015, 'Topology Optimization, Additive Layer Manufacturing, and Experimental Testing of an Air-Cooled Heat Sink', *Journal of Mechanical Design, Transactions of the ASME*, 137(11), pp. 1–9. doi: 10.1115/1.4030989.
- Deisenroth, D. C., Moradi, R., Shooshtari, A. H., Singer, F., Bar-Cohen, A., Ohadi, M., 2018, 'Review of Heat Exchangers Enabled by Polymer and Polymer Composite Additive Manufacturing', *Heat Transfer Engineering*. Taylor & Francis, 39(19), pp. 1652–1668. doi: 10.1080/01457632.2017.1384280.
- Glade, H., Moses, D. and Orth, T., 2017, 'Polymer composite heat exchangers', *Innovative Heat Exchangers*, pp. 53–116. doi: 10.1007/978-3-319-71641-1_2.
- Heinle, C. and Drummer, D., 2010, 'Potential of thermally conductive polymers for the cooling of mechatronic parts', *Physics Procedia*, 5(PART 2), pp. 735–744. doi: 10.1016/j.phpro.2010.08.106.
- Icoz, T. and Arik, M., 2010, 'Light weight high performance thermal management with advanced heat sinks and extended surfaces', *IEEE Transactions on Components and Packaging Technologies*. IEEE, 33(1), pp. 161–166. doi: 10.1109/TCAPT.2009.2026736.
- Joo, Y. and Kim, S. J., 2015, 'Comparison of thermal performance between plate-fin and pin-fin heat sinks in natural convection', *International Journal of Heat and Mass Transfer*. Elsevier Ltd, 83, pp. 345–356. doi: 10.1016/j.ijheatmasstransfer.2014.12.023.
- Kang, M. K., Shin, J. H., Lee, H. H., Chun, K., 2005, 'Analysis of laminar convective heat transfer in micro heat exchanger for stacked multi-chip module', *Microsystem Technologies*, 11(11), pp. 1176–1186. doi: 10.1007/s00542-005-0590-9.
- Koşar, A., 2010, 'Effect of substrate thickness and material on heat transfer in microchannel heat sinks', *International Journal of Thermal Sciences*, 49(4), pp. 635–642. doi: 10.1016/j.ijthermalsci.2009.11.004.
- Koyuncuoğlu, A., Okutucu, T. and Kūlah, H., 2010, 'A CMOS compatible metal-polymer microchannel heat sink for monolithic chip cooling applications', 2010 14th International Heat Transfer Conference, IHTC 14, 3(January), pp. 721–724. doi: 10.1115/IHTC14-23212.

- Lee, H., Jeong, Y., Shin, J., Baek, J., Kang, M., Chun, K., 2004, 'Package embedded heat exchanger for stacked multi-chip module', *Sensors and Actuators, A: Physical*, 114(2–3), pp. 204–211. doi: 10.1016/j.sna.2003.12.026.
- Lee, H., 2017, *Thermal design*. 2nd edn, HEDH Multimedia. 2nd edn. JohnWiley & Sons, Inc. doi: 10.1615/hedhme.a.000278.
- Lee, T. H., Park, J. H., Kim, J. U., Cho, H. G., 2013, 'Thermal properties and temperature distribution of epoxy composite with micro and nano AlN for molded transformer', *Proceedings of IEEE International Conference on Solid Dielectrics, ICSD*. IEEE, pp. 927–930. doi: 10.1109/ICSD.2013.6619693.
- Marchetto, D., Carneiro Moreira, D. and Ribatski, G., 2019, 'A Review on Polymer Heat Sinks for Electronic Cooling Applications', (April 2019). doi: 10.26678/abcm.encit2018.cit18-0394.
- Marotta, E. E., Ellsworth, M. J., Norley, J., Getz, G., 2003, 'The Development of a Bonded Fin Graphite/Epoxy Heat Sink for High Performance Servers', *Advances in Electronic Packaging*, 2(Mcm), pp. 139–146. doi: 10.1115/ipack2003-35060.
- Nafis, B. M., Whitt, R., Iradukunda, A. C., Huitink, D., 2021, 'Additive Manufacturing for Enhancing Thermal Dissipation in Heat Sink Implementation: A Review', *Heat Transfer Engineering*. Taylor & Francis, 42(12), pp. 967–984. doi: 10.1080/01457632.2020.1766246.
- Norley, J., Tzeng, J. J.W., Getz, G., Klug, J., Fedor, B., 2001, 'The development of a natural graphite heat-spreader', *Annual IEEE Semiconductor Thermal Measurement and Management Symposium*, pp. 107–110. doi: 10.1109/stherm.2001.915157.
- Ong, Y. S. and KuShaari, K. Z., 2020, 'CFD investigation of the feasibility of polymer-based microchannel heat sink as thermal solution', *Chinese Journal of Chemical Engineering*. Elsevier B.V., 28(4), pp. 980–994. doi: 10.1016/j.cjche.2020.01.007.
- Smalc, M., Chen, G., Shives, G., Guggari, S., Iii, A. R., Norley, J., 2005, 'THERMAL PERFORMANCE OF NATURAL GRAPHITE HEAT SPREADERS', *Proceedings of IPACK2005*, pp. 1–11.
- Subramaniam, V., Dbouk, T. and Harion, J. L., 2018, 'Topology optimization of conductive heat transfer devices: An experimental investigation', *Applied Thermal Engineering*. Elsevier Ltd, 131, pp. 390–411. doi: 10.1016/j.applthermaleng.2017.12.026.
- Waheed, S., Cabot, J. M., Smejkal, P., Farajikhah, S., Sayyar, S., Innis, P. C., Beirne, S., Barnsley, G., Lewis, T. W., Breadmore, M. C., Paull, Brett, 2019, 'Three-Dimensional Printing of Abrasive, Hard, and Thermally Conductive Synthetic Microdiamond-Polymer Composite Using Low-Cost Fused Deposition Modeling Printer', *ACS Applied Materials and Interfaces*, 11(4), pp. 4353–4363. doi: 10.1021/acsami.8b18232.
- Wong, M., Owen, I., Sutcliffe, C. J., Puri, A., 2009, 'Convective heat transfer and pressure losses across novel heat sinks fabricated by Selective Laser Melting', *International Journal of Heat and Mass Transfer*. Elsevier Ltd, 52(1–2), pp. 281–288. doi: 10.1016/j.ijheatmasstransfer.2008.06.002.

ACKNOWLEDGEMENT

This article was developed within the scope of the “Agenda/Alianças Verdes para a Inovação Empresarial” by the Consortium “NGS New Generation Storage” co-financed by NextGenerationEU, through the 'Business Innovation Agendas' investment from the Recovery and Resilience Plan (RRP).

